E1.17-0021-18

Search for GeV gamma-ray counterparts of gravitational wave events by CALET

Masaki Mori (Ritsumeikan University)

Yoichi Asaoka (Waseda University)

for the CALET collaboration

Accepted for publication in ApJ

42nd COSPAR Assembly, July 14-22, 2018, Pasadena, CA

Electromagnetic emission from Gravitational Events?

Yes	No?
• NS-NS binary mergers • NS-BH binary mergers? (e.g. Phinney 2009, Rosswog 2016, Fernández&Metzger 2016)	• BH-BH binary mergers (e.g. De Mink&King 2017)

GW170817 (~1.5$M_\odot$+~1.3$M_\odot$)
+ EM emission + GRB 170817A

GW150914 (36$M_\odot$+29$M_\odot$)
GW151226 (14$M_\odot$+7.5$M_\odot$)
GW170104 (31$M_\odot$+19$M_\odot$)
GW170608 (12$M_\odot$+7$M_\odot$)
GW170814 (31$M_\odot$+25$M_\odot$)

CALET

Wide field-of-view monitors are necessary to detect prompt EM emission

CALET/CAL is watching for ~1/6 of the whole sky!

CALorimetric Electron Telescope

Launch: Aug. 19, 2015
by Japanese H-IIB

CALET Gamma ray Burst Monitor (CGBM)

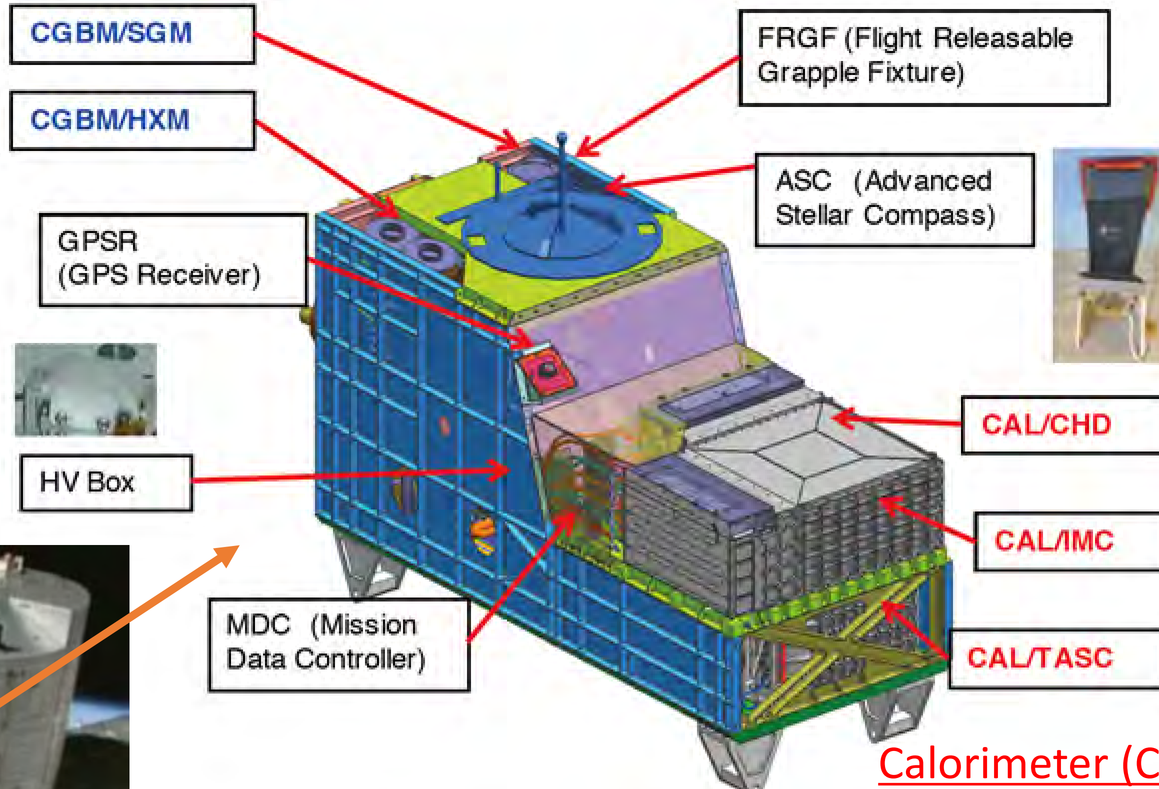

Calorimeter (CAL)

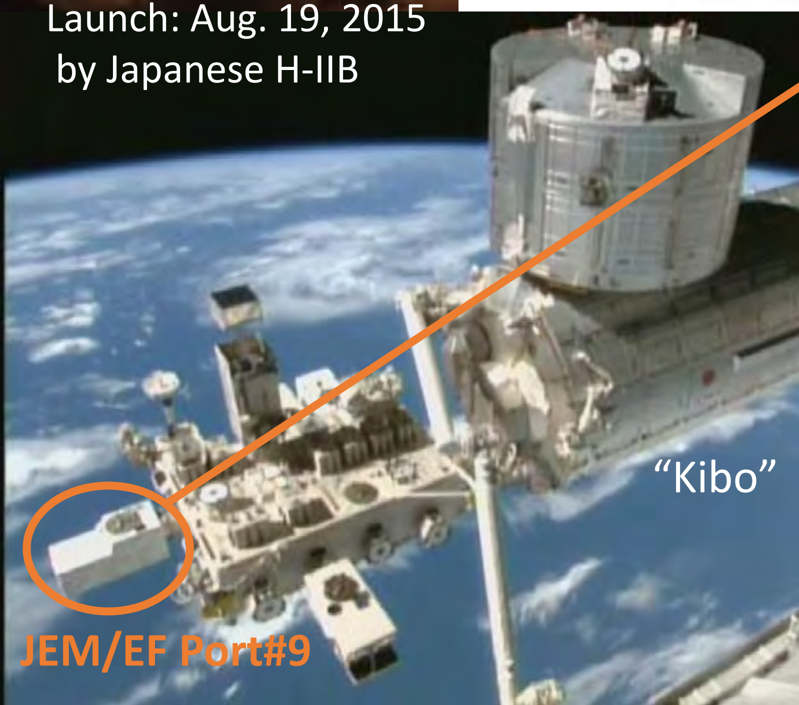

- Mass: 612.8kg
- JEM standard payload size:
  1850mm(L) x 800mm(W) x 1000mm(H)
- Power consumption: 507 W (max)
- Telemetry:
  Medium 600 kbps (6.5GB/day) / Low 50 kbps

(JEM : Japanese Experiment Module "Kibo" on ISS)

CALET Collaboration Team

O. Adriani[25], Y. Akaike[2], K. Asano[7], Y. Asaoka[9,31], M.G. Bagliesi[29], E. Berti[25], G. Bigongiari[29], W.R. Binns[32], S. Bonechi[29], M. Bongi[25], P. Brogi[29], A. Bruno[15], J.H. Buckley[32], N. Cannady[13], G. Castellini[25], C. Checchia[26],M.L. Cherry[13], G. Collazuol[26], V. Di Felice[28], K. Ebisawa[8], H. Fuke[8], T.G. Guzik[13], T. Hams[3], N. Hasebe[31], K. Hibino[10], M. Ichimura[4], K. Ioka[34], W. Ishizaki[7], M.H. Israel[32], K. Kasahara[31], J. Kataoka[31], R. Kataoka[17], Y. Katayose[33], C. Kato[23], Y.Kawakubo[1], N. Kawanaka[30], K. Kohri [12], H.S. Krawczynski[32], J.F. Krizmanic[2], T. Lomtadze[27], P. Maestro[29], P.S. Marrocchesi[29], A.M. Messineo[27], J.W. Mitchell[15], S. Miyake[5], A.A. Moiseev[3], K. Mori[9,31], M. Mori[20], N. Mori[25], H.M. Motz[31], K. Munakata[23], H. Murakami[31], S. Nakahira[9], J. Nishimura[8], G.A De Nolfo[15], S. Okuno[10], J.F. Ormes[25], S. Ozawa[31], L. Pacini[25], F. Palma[28], V. Pal'shin[1], P. Papini[25], A.V. Penacchioni[29], B.F. Rauch[32], S.B. Ricciarini[25], K. Sakai[3], T. Sakamoto[1], M. Sasaki[3], Y. Shimizu[10], A. Shiomi[18], R. Sparvoli[28], P. Spillantini[25], F. Stolzi[29], S. Sugita[1], J.E. Suh[29], A. Sulaj[29], I. Takahashi[11], M. Takayanagi[8], M. Takita[7], T. Tamura[10], N. Tateyama[10], T. Terasawa[7], H. Tomida[8], S. Torii[31], Y. Tunesada[19], Y. Uchihori[16], S. Ueno[8], E. Vannuccini[25], J.P. Wefel[13], K. Yamaoka[14], S. Yanagita[6], A. Yoshida[1], and K. Yoshida[22]

1) Aoyama Gakuin University, Japan
2) CRESST/NASA/GSFC and Universities Space Research Association, USA
3) CRESST/NASA/GSFC and University of Maryland, USA
4) Hirosaki University, Japan
5) Ibaraki National College of Technology, Japan
6) Ibaraki University, Japan
7) ICRR, University of Tokyo, Japan
8) ISAS/JAXA Japan
9) JAXA, Japan
10) Kanagawa University, Japan
11) Kavli IPMU, University of Tokyo, Japan
12) KEK, Japan
13) Louisiana State University, USA
14) Nagoya University, Japan
15) NASA/GSFC, USA
16) National Inst. of Radiological Sciences, Japan
17) National Institute of Polar Research, Japan
18) Nihon University, Japan
19) Osaka City University, Japan
20) Ritsumeikan University, Japan
21) Saitama University, Japan
22) Shibaura Institute of Technology, Japan
23) Shinshu University, Japan
24) University of Denver, USA
25) University of Florence, IFAC (CNR) and INFN, Italy
26) University of Padova and INFN, Italy
27) University of Pisa and INFN, Italy
28) University of Rome Tor Vergata and INFN, Italy
29) University of Siena and INFN, Italy
30) University of Tokyo, Japan
31) Waseda University, Japan
32) Washington University-St. Louis, USA
33) Yokohama National University, Japan
34) Yukawa Institute for Theoretical Physics, Kyoto University, Japan

CALET/CAL Detector

Fully active thick calorimeter ($30X_0$) optimized for electron spectrum measurements well into TeV region

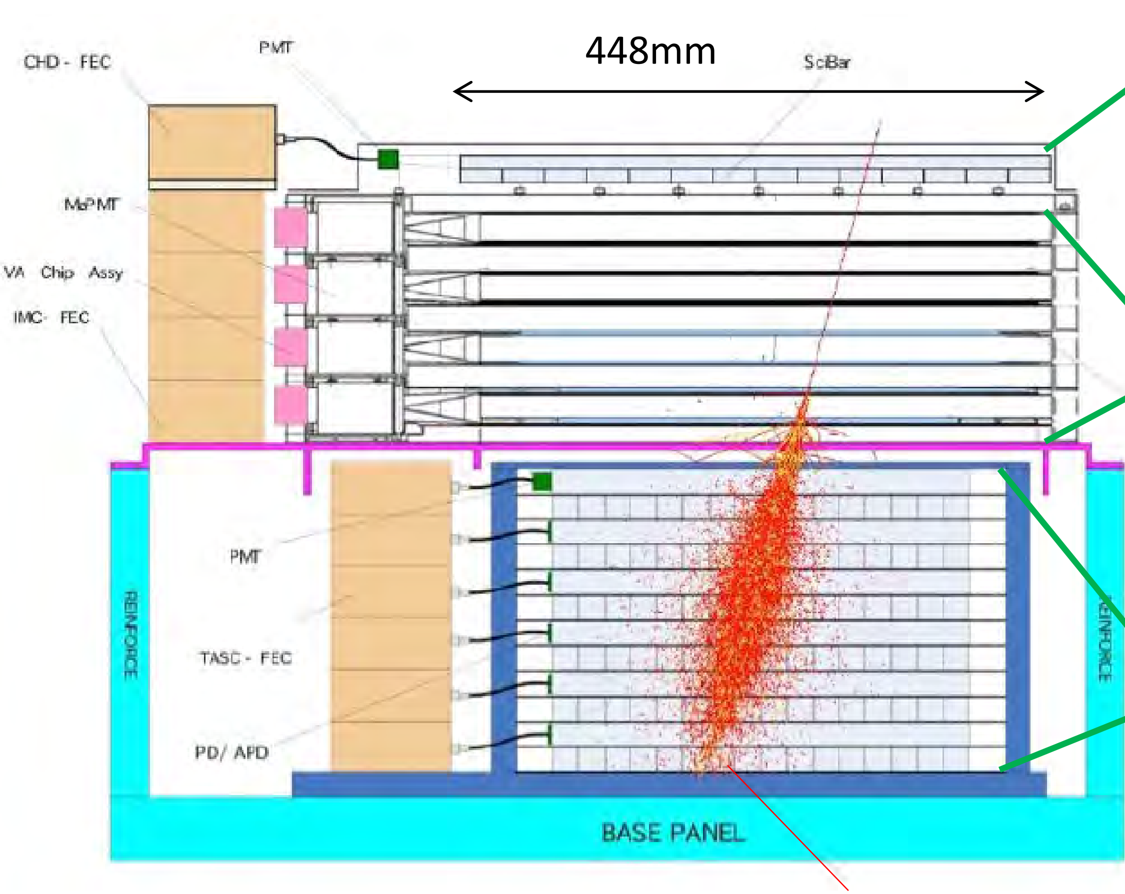

1TeV electron shower is fully contained in TASC

Charge Detector **CHD**

plastic scintillator hodoscope,
absolute charge measurement
(including charge zero)

Imaging Calorimeter **IMC**

SciFi + tungsten plate ($3X_0$),
reconstruction of arrival direction and initial shower development

Total Absorption Calorimeter **TASC**

PWO hodoscope ($27X_0$),
energy measurements and particle identification

Overview of CALET/CAL Trigger System

Y. Asaoka et al., Astroparticle Phys. 100, 29 (2018)

High Energy Shower Trigger (HE)

- High energy electrons (10GeV ～20TeV)
- High energy gamma rays (10GeV ～10TeV)
- Nuclei (a few10GeV～1000TeV)

Low Energy Shower Trigger (LE)

- Low energy electron at high latitude (1GeV ～10GeV)
- GeV gamma-rays originated from GRB (1GeV ～)
- Ultra heavy nuclei (combined with heavy mode)

Single Trigger (Single)

- For detector calibration : penetrating particles
  (mainly non-interacting protons and heliums)

(*) In addition to above 3 trigger modes, heavy modes are defined for each of the above trigger mode. They are omitted here for simple explanation.

Auto Trigger (Pedestal/Test Pulse)

- For calibration:
  - ADC offset measurement (Pedestal)
  - FEC's response measurement (Test pulse)

ISS Orbit and CALET Operations

Y. Asaoka et al., Astroparticle Phys. 100, 29 (2018)

ISS orbit: inclination 51.6 degree, ~400 km

Concept of on-orbit operations

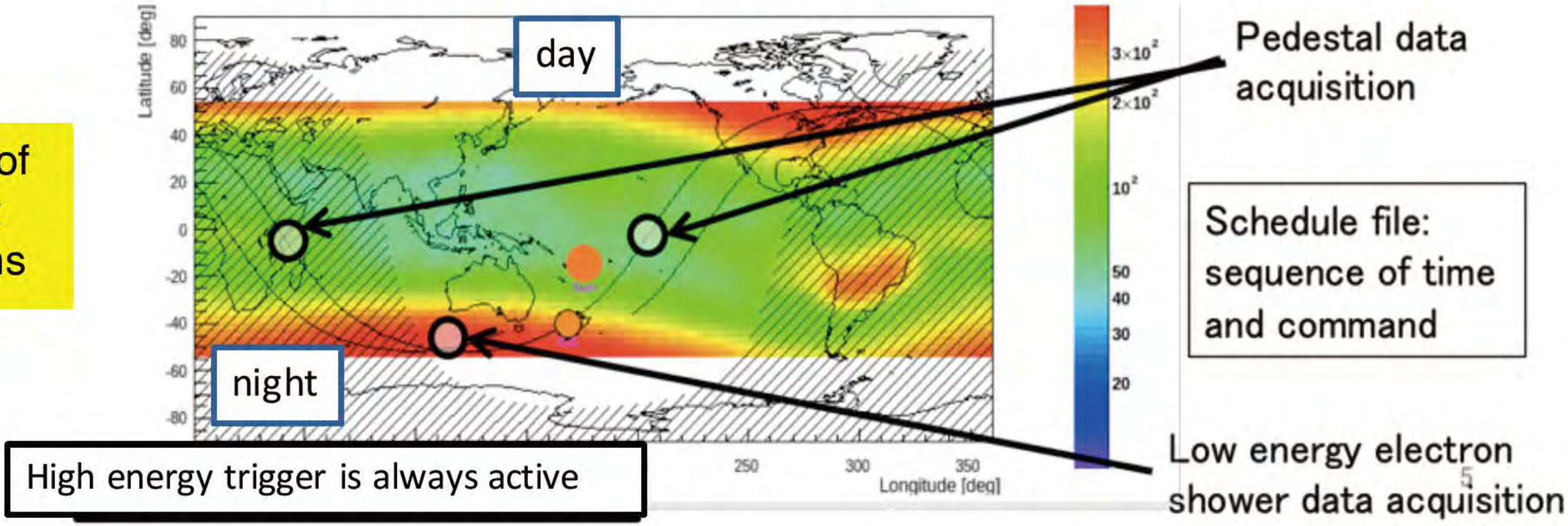

Dependence of the count rate on geomagnetic latitude

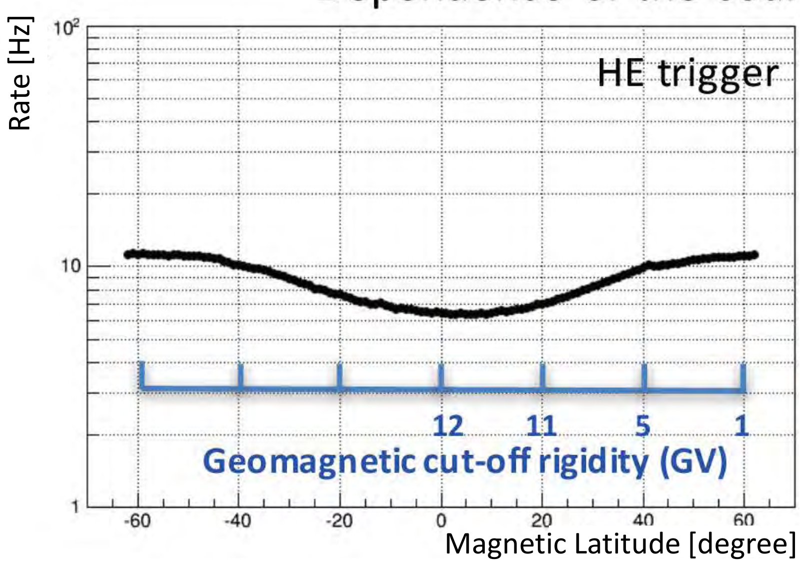

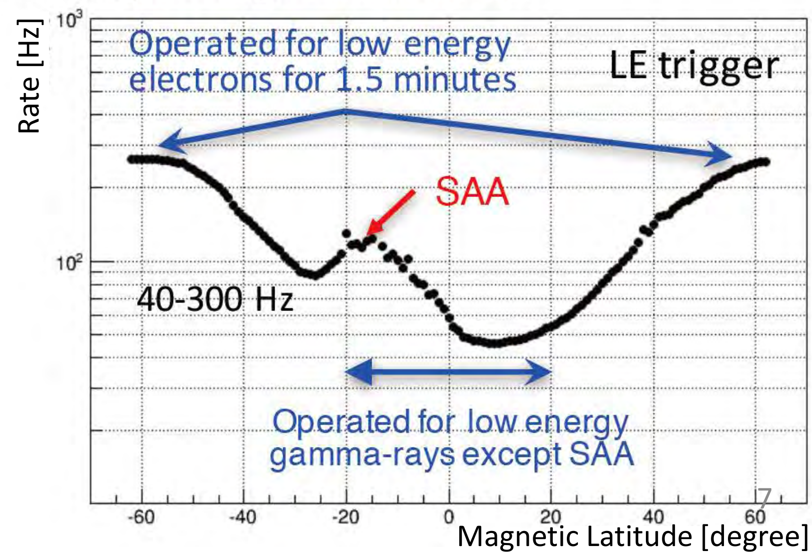

CAL Limit Calculation Procedure

Gamma-ray Event Selection

Lower energy is important

Effective Area Calculation

S_{eff} as a function of zenith and azimuth

Exposure Calculation

S_{eff}(zen,azi) T_{live} projected to sky event by event along the ISS (CALET) orbit

Upper Limit Calculation

If no gamma-rays are observed

Check Overlap with LIGO Localization Map

Validation of Sensitivity with Observation of Diffuse/Point Sources

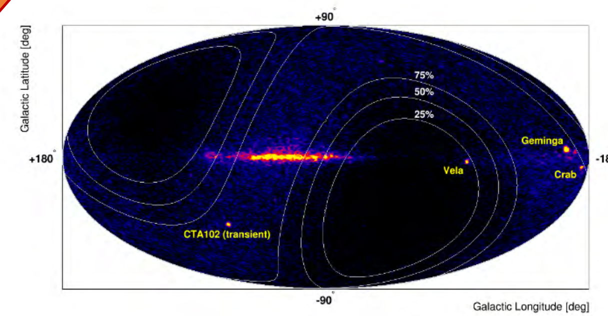

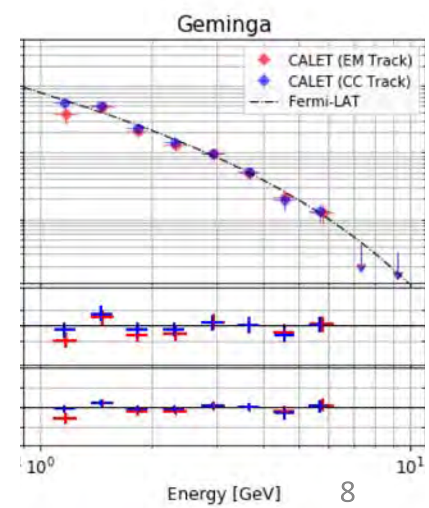

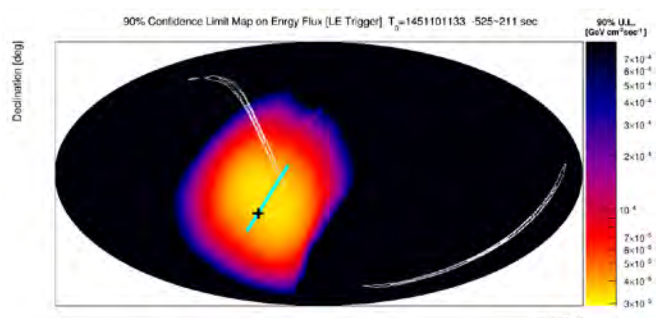

Gamma Ray Event Selection

= Electron Selection Cut + Gamma-ray ID Cut w/ Lower Energy Extension

<u>100 GeV Event Examples</u>

gamma-ray | electron | proton

Charge Z=0 | Charge Z=1

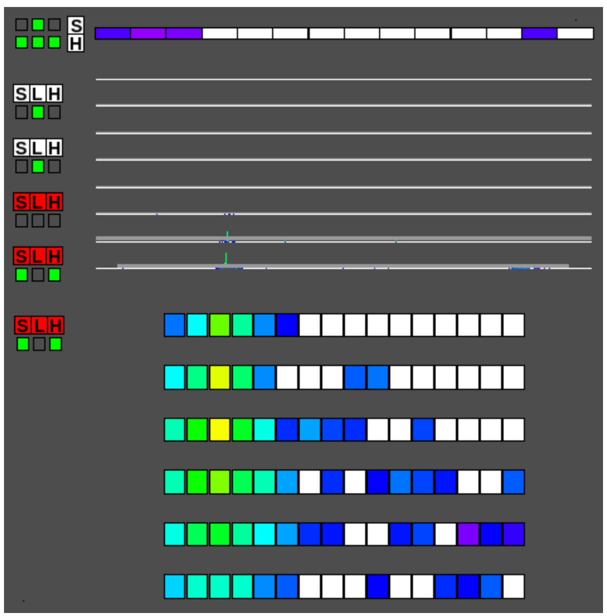

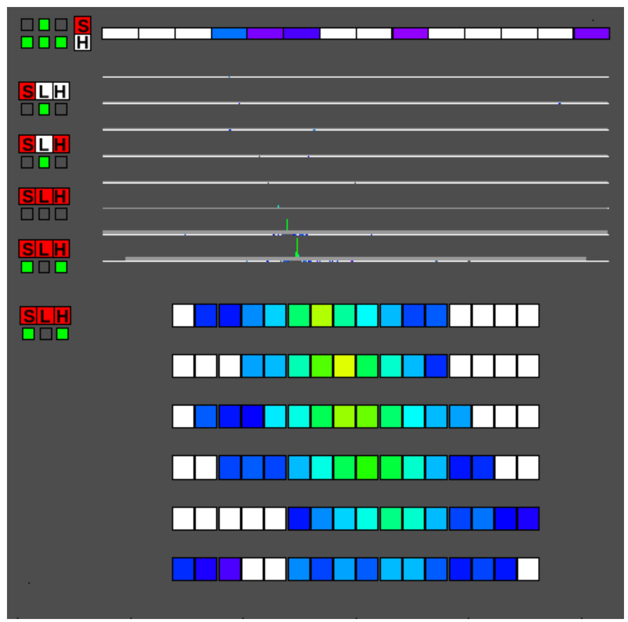

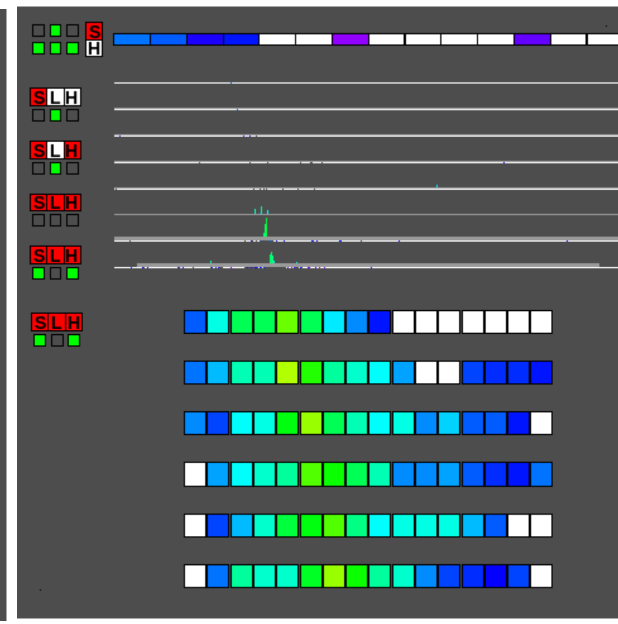

Electromagnetic Shower | Hadron Shower

well contained shower development

larger spread

Gamma Ray Event Selection

= Electron Selection Cut + Gamma-ray ID Cut w/ Lower Energy Extension

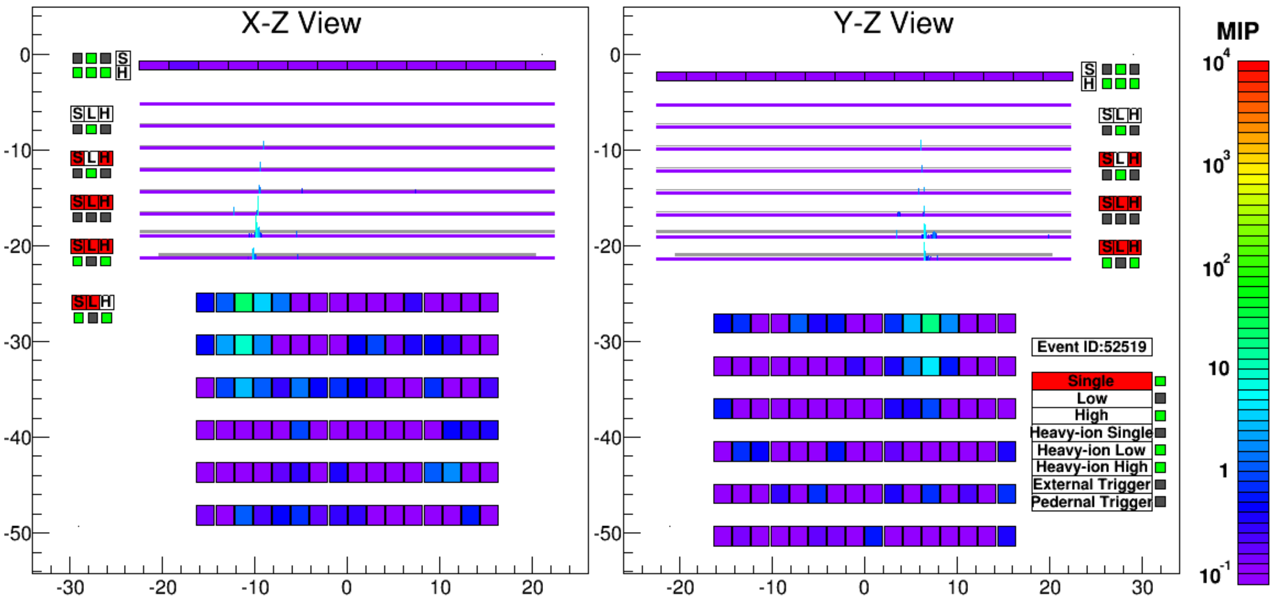

An example of gamma-ray event candidate in flight data (reconstructed primary energy ~5GeV)

1. Geometry Condition
   - CHD-Top to TASC 1^{st} layer (2cm margin)
2. Pre selection
   - Offline trigger
   - Shower concentration
   - Shower starting point
3. Track quality cut
   - Track hits >2
   - matching w/ TASC
4. Electromagnetic shower selection
   - shower shape
5. Gamma-ray ID
   - CHD/IMC-veto (combination of loose cuts)
6. FOV cut

Gamma Ray Event Selection

= Electron Selection Cut + Gamma-ray ID Cut w/ Lower Energy Extension

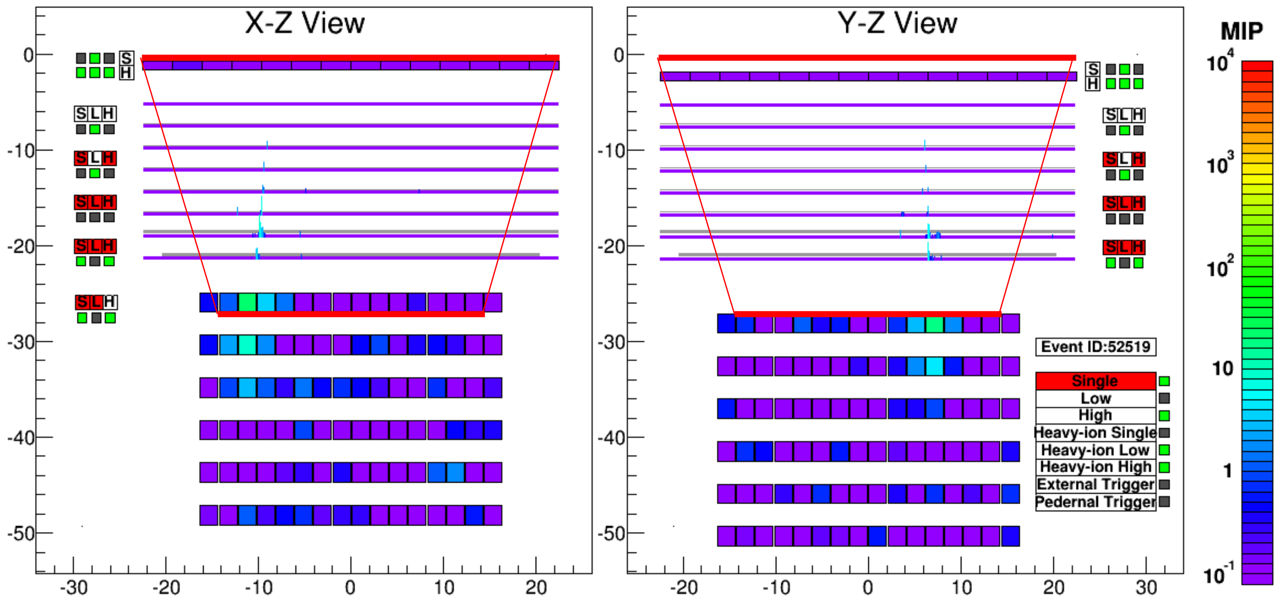

1. Geometry Condition
   - CHD-Top to TASC 1st layer (2cm margin)
2. Pre selection
   - Offline trigger
   - Shower concentration
   - Shower starting point
3. Track quality cut
   - Track hits >2
   - matching w/ TASC
4. Electromagnetic shower selection
   - shower shape
5. Gamma-ray ID
   - CHD/IMC-veto (combination of loose cuts)
6. FOV cut

To maximize the field of view (FOV), the requirements on acceptance condition was loosened as much as possible compared to electron analysis. However, penetration of CHD paddle by shower axis is required to ensure charge zero selection.

Gamma Ray Event Selection

= Electron Selection Cut + Gamma-ray ID Cut w/ Lower Energy Extension

"K-cut" $K = \log_{10}(F_E) + \frac{1}{2}R_E$

F_E : fractional energy deposit of TASC-Y6 relative to total TASC deposit

R_E : second moment of lateral energy deposit distribution relative to shower axis [cm]

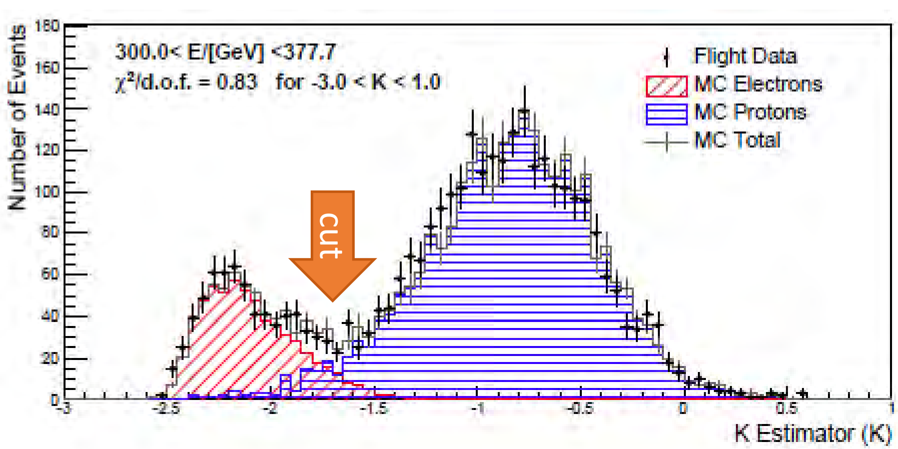

FIG. 2. An example of K-estimator distribution in the 300 < E < 378 GeV bin. The reduced chi-square of the fit in the K-estimator range from -3 to 1 is 0.83.

O. Adriani et al., PRL 119, 181101 (2017) supplemental material

1. Geometry Condition
   - CHD-Top to TASC 1st layer (2cm margin)
2. Pre selection
   - Offline trigger
   - Shower concentration
   - Shower starting point
3. Track quality cut
   - Track hits >2
   - matching w/ TASC
4. Electromagnetic shower selection
   - shower shape
5. Gamma-ray ID
   - CHD/IMC-veto (combination of loose cuts)
6. FOV cut

Gamma Ray Event Selection

= Electron Selection Cut + Gamma-ray ID Cut w/ Lower Energy Extension

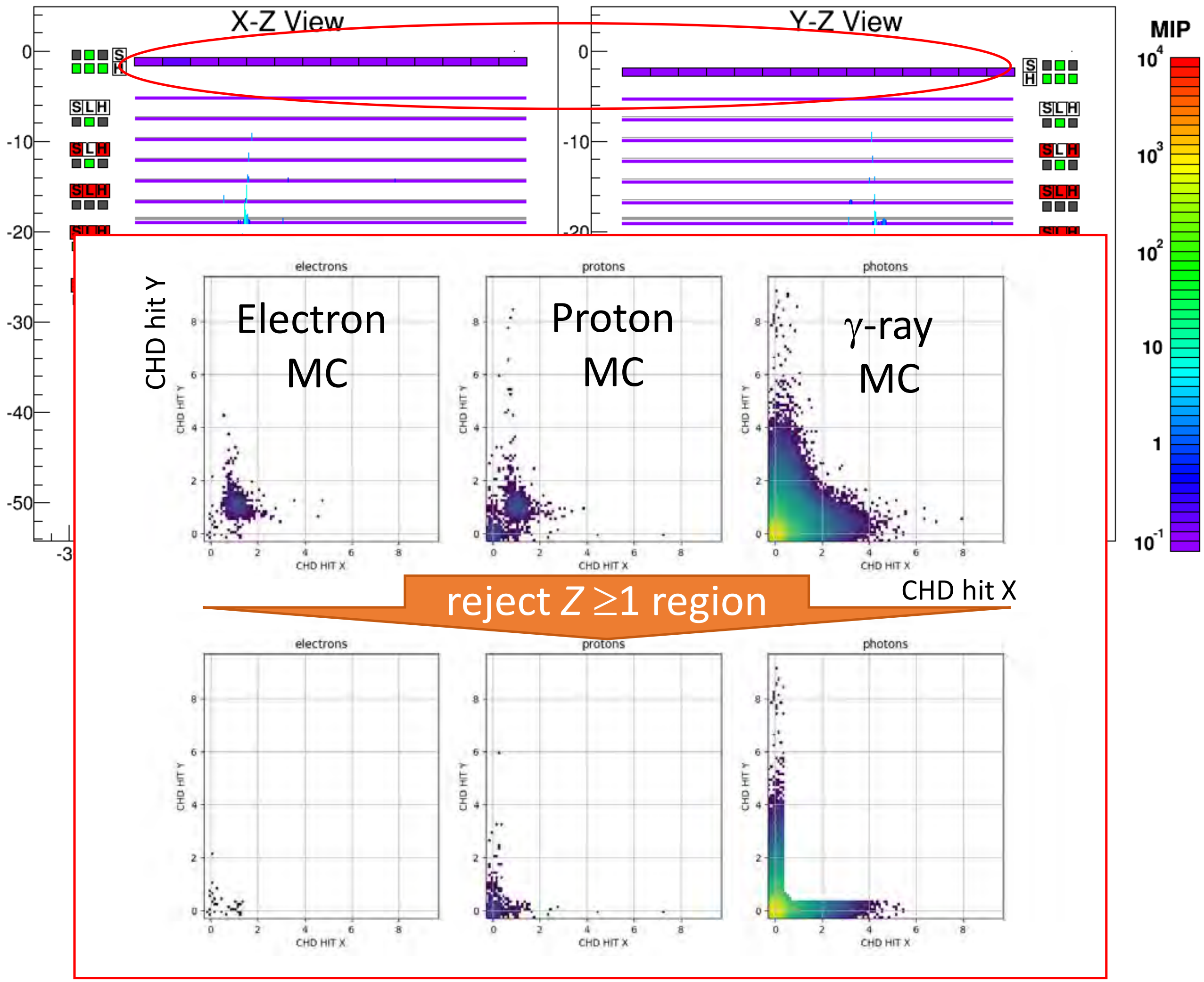

1. Geometry Condition
   - CHD-Top to TASC 1st layer (2cm margin)
2. Pre selection
   - Offline trigger
   - Shower concentration
   - Shower starting point
3. Track quality cut
   - Track hits >2
   - matching w/ TASC
4. Electromagnetic shower selection
   - shower shape
5. **Gamma-ray ID**
   - **CHD/IMC-veto (combination of loose cuts)**
6. FOV cut

Gamma Ray Event Selection

= Electron Selection Cut + Gamma-ray ID Cut w/ Lower Energy Extension

It was found that secondary gamma rays produced in ISS structures are dominant source of background

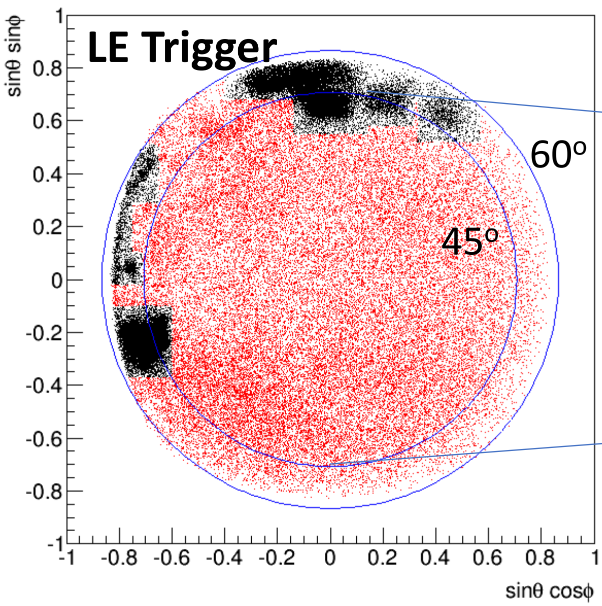

Gamma-ray candidates in CALET FOV

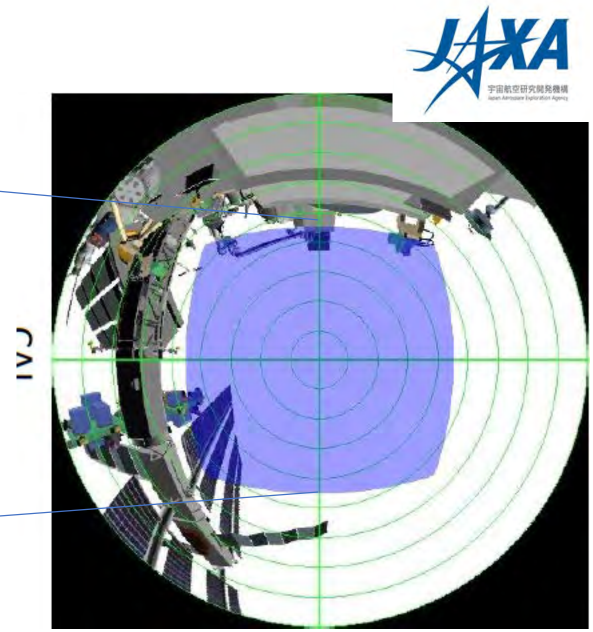

Fish-eye view of CALET FOV

By removing Black parts, it is possible to reject majority of such background. More sophisticated rejection method is under development.

1. Geometry Condition
   - CHD-Top to TASC 1st layer (2cm margin)
2. Pre selection
   - Offline trigger
   - Shower concentration
   - Shower starting point
3. Track quality cut
   - Track hits >2
   - matching w/ TASC
4. Electromagnetic shower selection
   - shower shape
5. Gamma-ray ID
   - CHD-veto
6. FOV cut

Effective Area and Sensitivity

Preliminary
O. Adriani et al., in prep.

Effective area is estimated as a function of incident angle (dx/dz, dy/dz) and energy. Maximum effective area is achieved at around 5 GeV, but lower energy is more important for steep spectrum like E^{-2}.

3-10GeV average

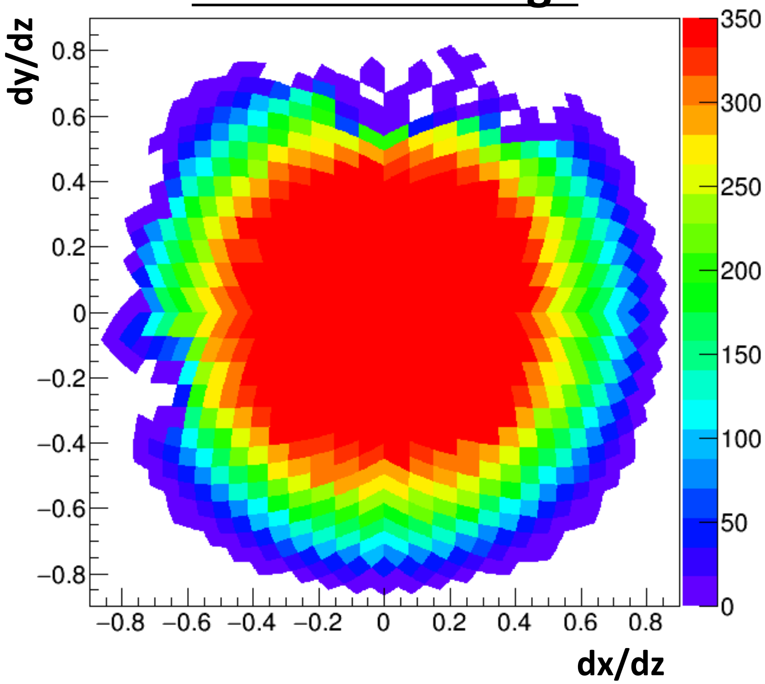

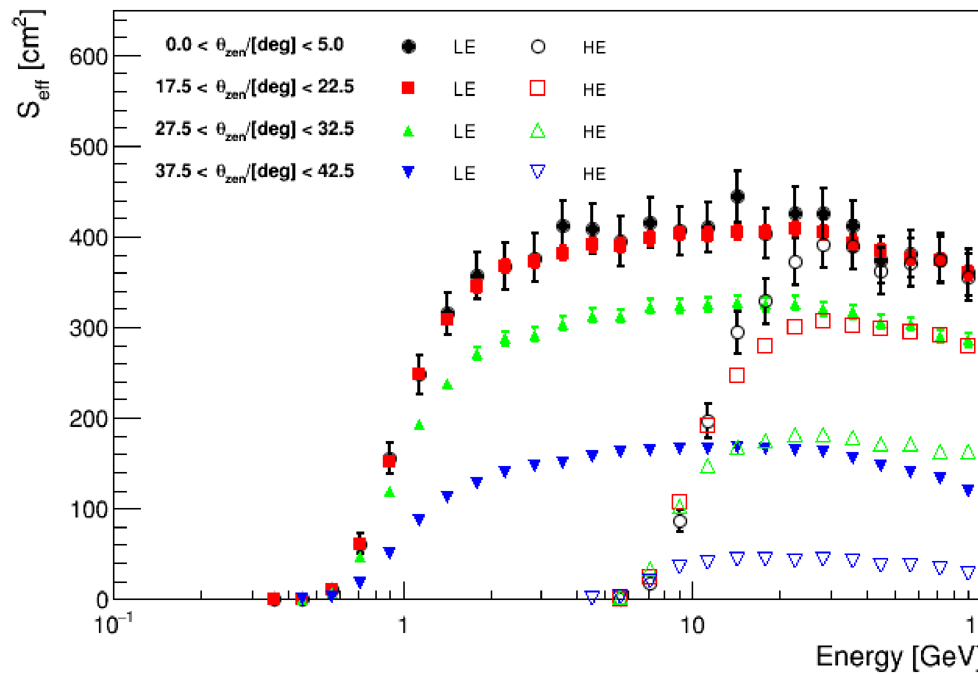

Mostly axially symmetric except for FOV cut

Effective area as a function of energy. Four representative zenith angle ranges are shown.

GW Counterpart Search with CALET

The Astrophysical Journal Letters, 829:L20 (5pp), 2016 September 20
doi:10.3847/2041-8205/829/1/L20

CrossMark

CALET UPPER LIMITS ON X-RAY AND GAMMA-RAY COUNTERPARTS OF GW151226

O. Adriani[1,2,3], Y. Akaike[4,5], K. Asano[6], Y. Asaoka[7,8], M. G. Bagliesi[2,9], G. Bigongiari[2,9], W. R. Binns[10], S. Bonechi[2,9], M. Bongi[1,2,3], P. Brogi[2,9], J. H. Buckley[10], N. Cannady[11], G. Castellini[1,2,3], C. Checchia[12], M. L. Cherry[11], G. Collazuol[12], V. Di Felice[2,13], K. Ebisawa[14], H. Fuke[14], T. G. Guzik[11], T. Hams[5,15], M. Hareyama[16], N. Hasebe[8], K. Hibino[17], M. Ichimura[18], K. Ioka[19], W. Ishizaki[6], M. H. Israel[10], A. Javaid[11], K. Kasahara[8], J. Kataoka[8], R. Kataoka[20], Y. Katayose[21], C. Kato[22], N. Kawanaka[23], Y. Kawakubo[24], H. Kitamura[25], H. S. Krawczynski[10], J. F. Krizmanic[4,5], S. Kuramata[18], T. Lomtadze[26], P. Maestro[2,9], P. S. Marrocchesi[2,9], A. M. Messineo[26], J. W. Mitchell[27], S. Miyake[28], K. Mizutani[29], A. A. Moiseev[5,30], K. Mori[8,14], M. Mori[31], N. Mori[1,2,3], H. M. Motz[32], K. Munakata[22], H. Murakami[8], Y. E. Nakagawa[14], S. Nakahira[7], J. Nishimura[14], S. Okuno[17], J. F. Ormes[33], S. Ozawa[8], L. Pacini[1,2,3], F. Palma[2,13], P. Papini[1,2,3], A. V. Penacchioni[9,34], B. F. Rauch[10], S. Ricciarini[1,2,3], K. Sakai[5,15], T. Sakamoto[24], M. Sasaki[5,30], Y. Shimizu[17], A. Shiomi[35], R. Sparvoli[2,13], P. Spillantini[1,2,3], F. Stolzi[2,9], I. Takahashi[36], M. Takayanagi[14], M. Takita[6], T. Tamura[17], N. Tateyama[17], T. Terasawa[37], H. Tomida[14], S. Torii[7,8], Y. Tsunesada[38], Y. Uchihori[25], S. Ueno[14],

Published in ApJ Letters

GW 151226 [B. P. Abbott *et al.*, PRL 116 (2016) 241103]

- GW trigger Time: 2015/12/26 3:38:53.647 UT
  - **gravitational-wave signal** produced by the coalescence of two stellar-mass black holes at a luminosity distance of ~440Mpc.

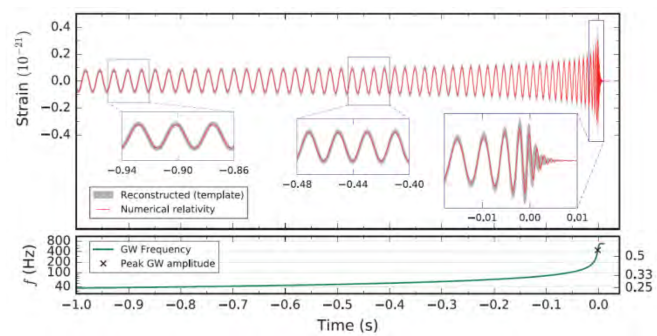

CALET Observation

- CGBM HV-on (3:20 – 3:40 UT)
  - No on-board trigger
- CAL: low-energy gamma-ray mode (> 1GeV) 3:30-3:43UT

Analysis update

- EM Track … developed and used extensively for electron analysis
- CC Track … developed specifically for low energy gamma-rays

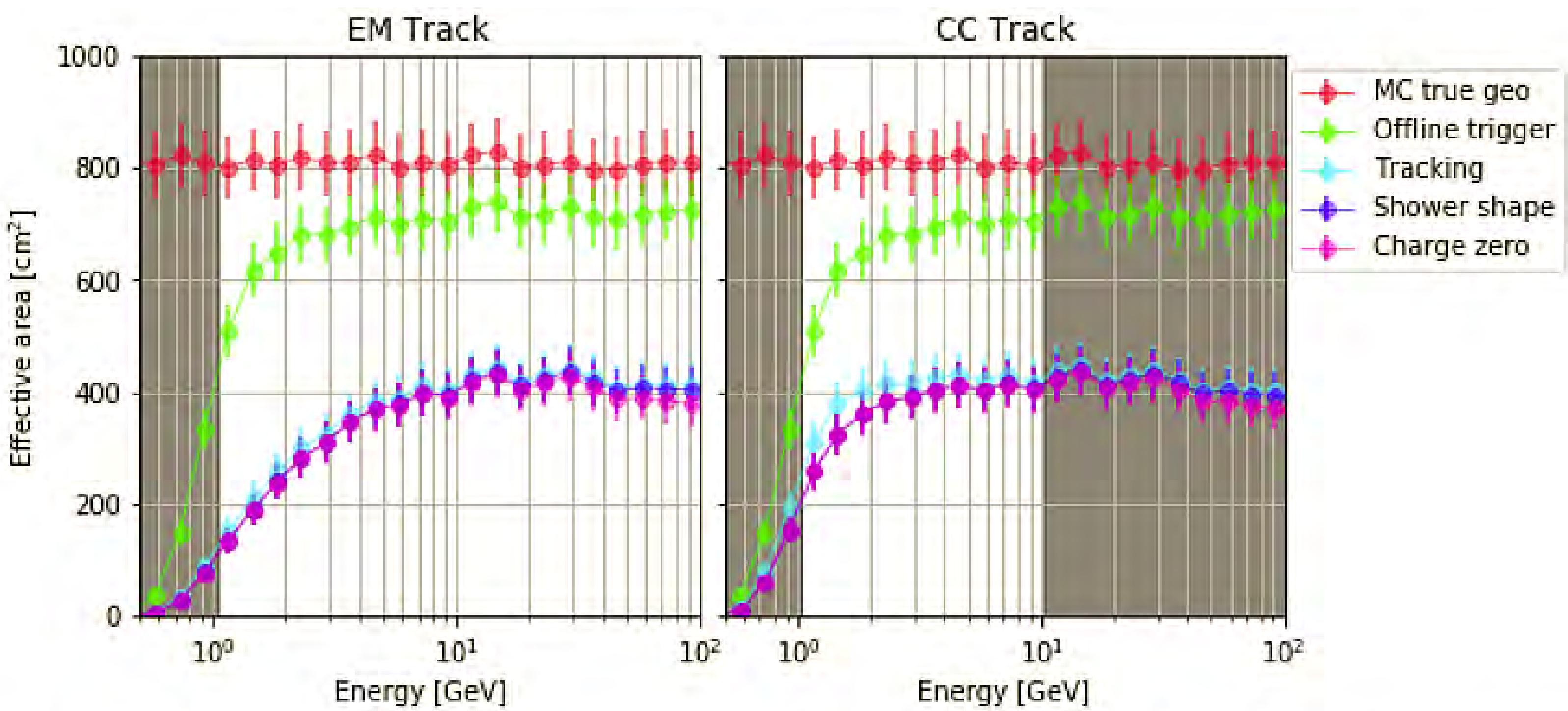

Figure 3. Effect of various selection cuts in zenith-pointing effective area. Grey shaded regions demonstrate the limits of applicability for each track due to background contamination with poor agreement between flight data and simulation.

90% CL Upper limit for GW151226 counterpart search

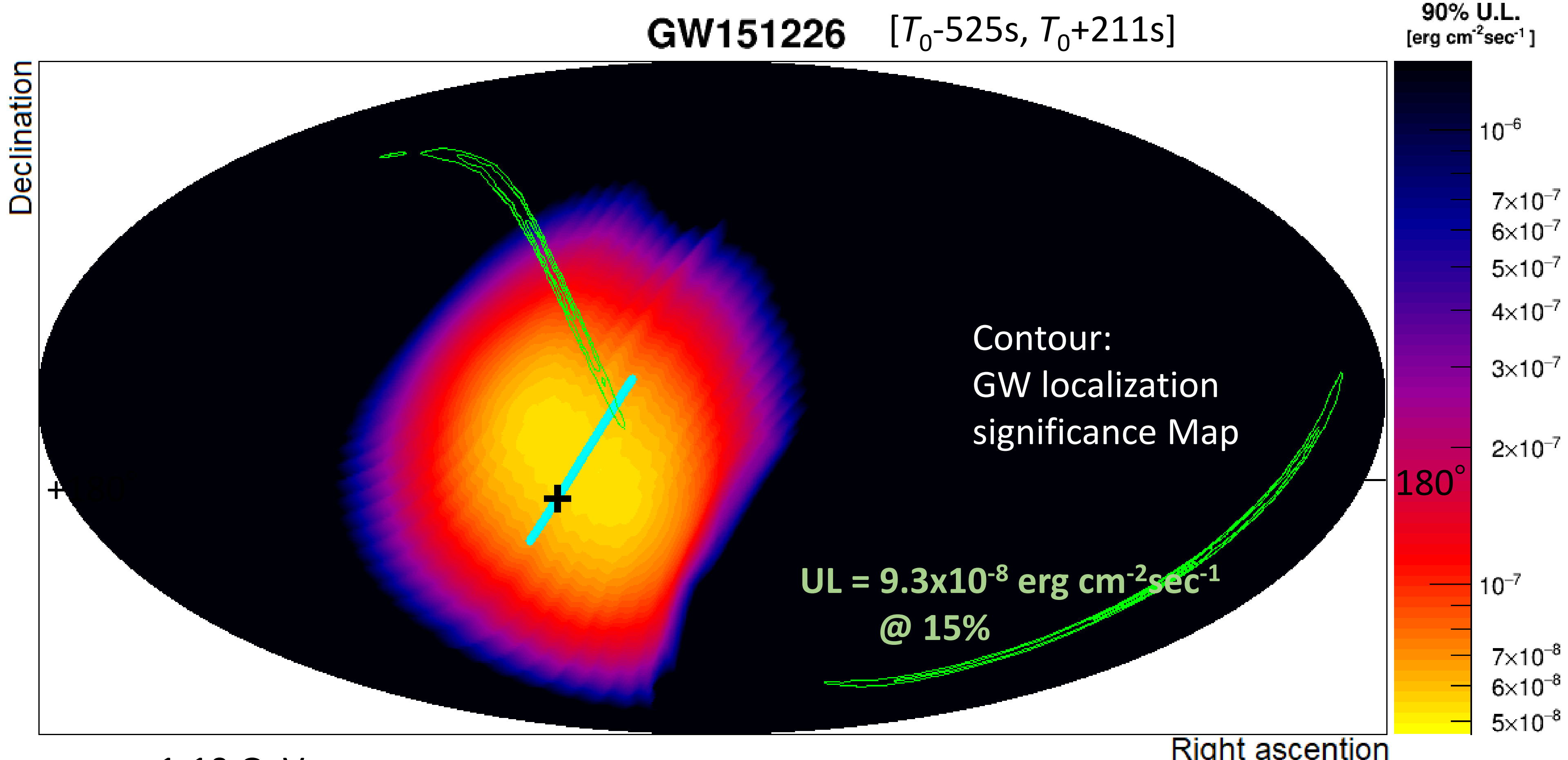

1-10 GeV

No event survived. Backgrounds are negligible.

CALET observation constrains at least some portion of LIGO probability.

90% CL Upper limit for GW170104 counterpart search

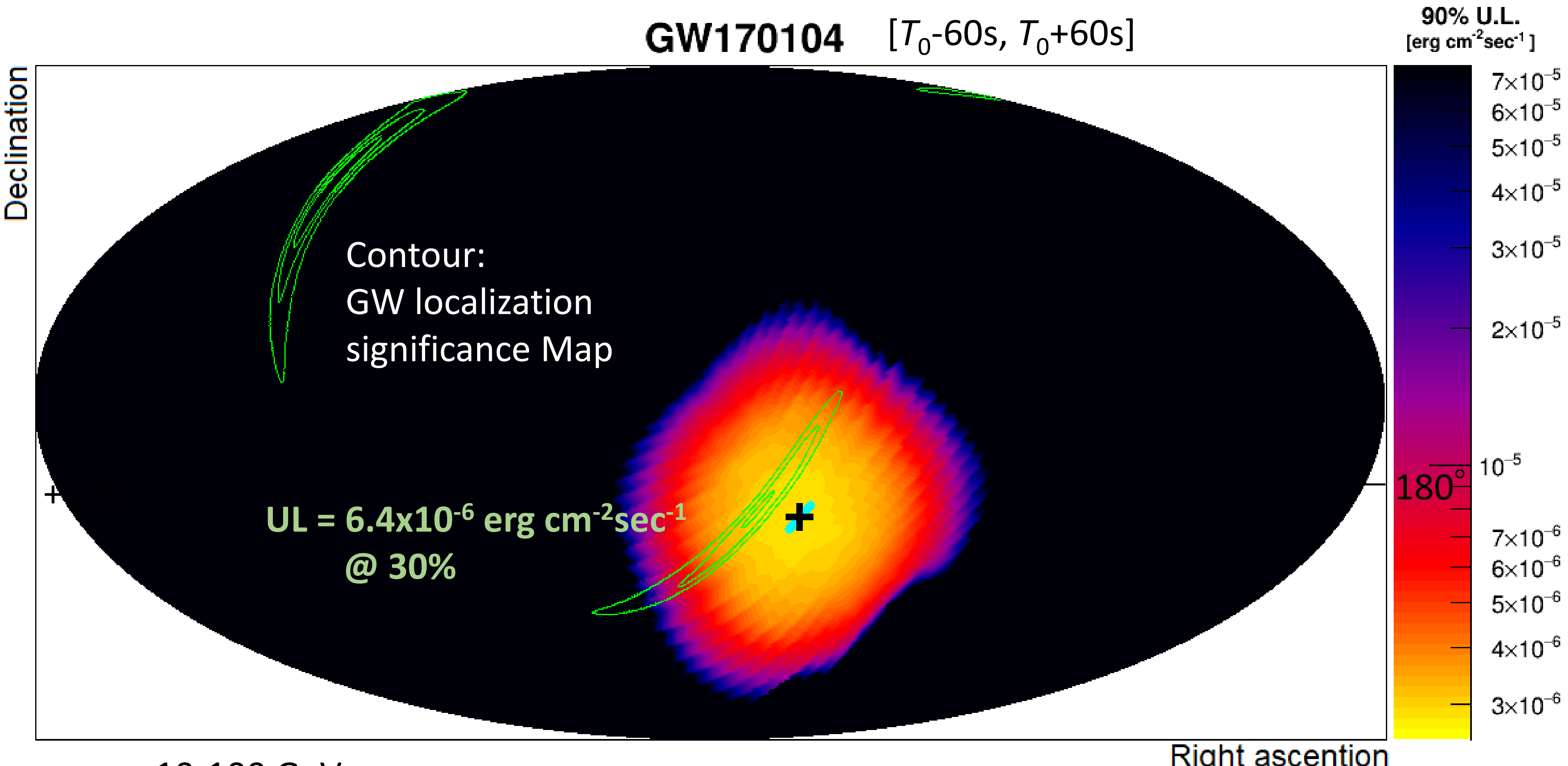

10-100 GeV

No event survived. Backgrounds are negligible.

CALET observation constrains at least some portion of LIGO probability.

90% CL Upper limit for GW170608 counterpart search

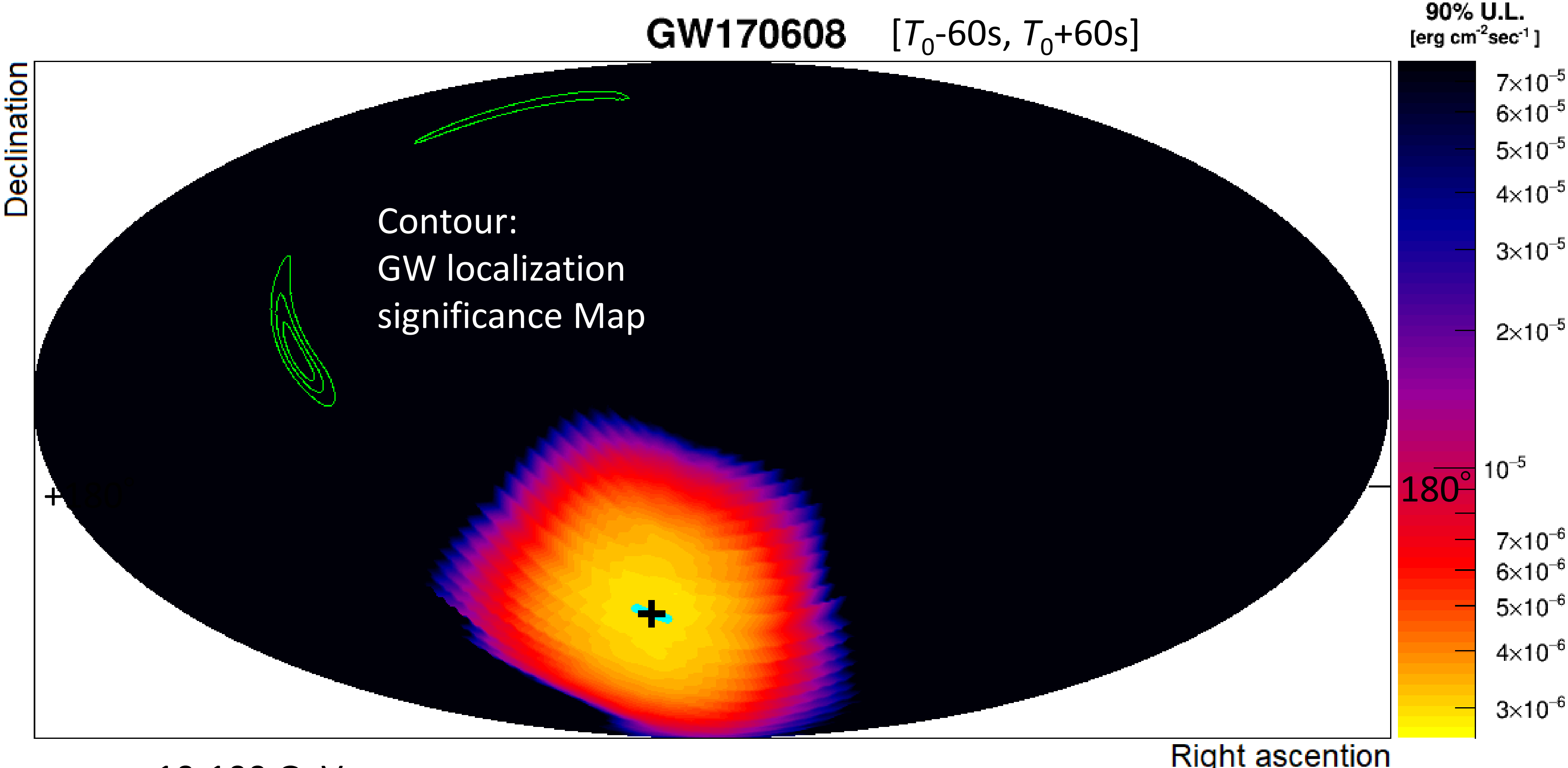

<u>10-100 GeV</u>

No event survived. Backgrounds are negligible.

CALET observation does not constrain any portion of LIGO probability.

90% CL Upper limit for GW170814 counterpart search

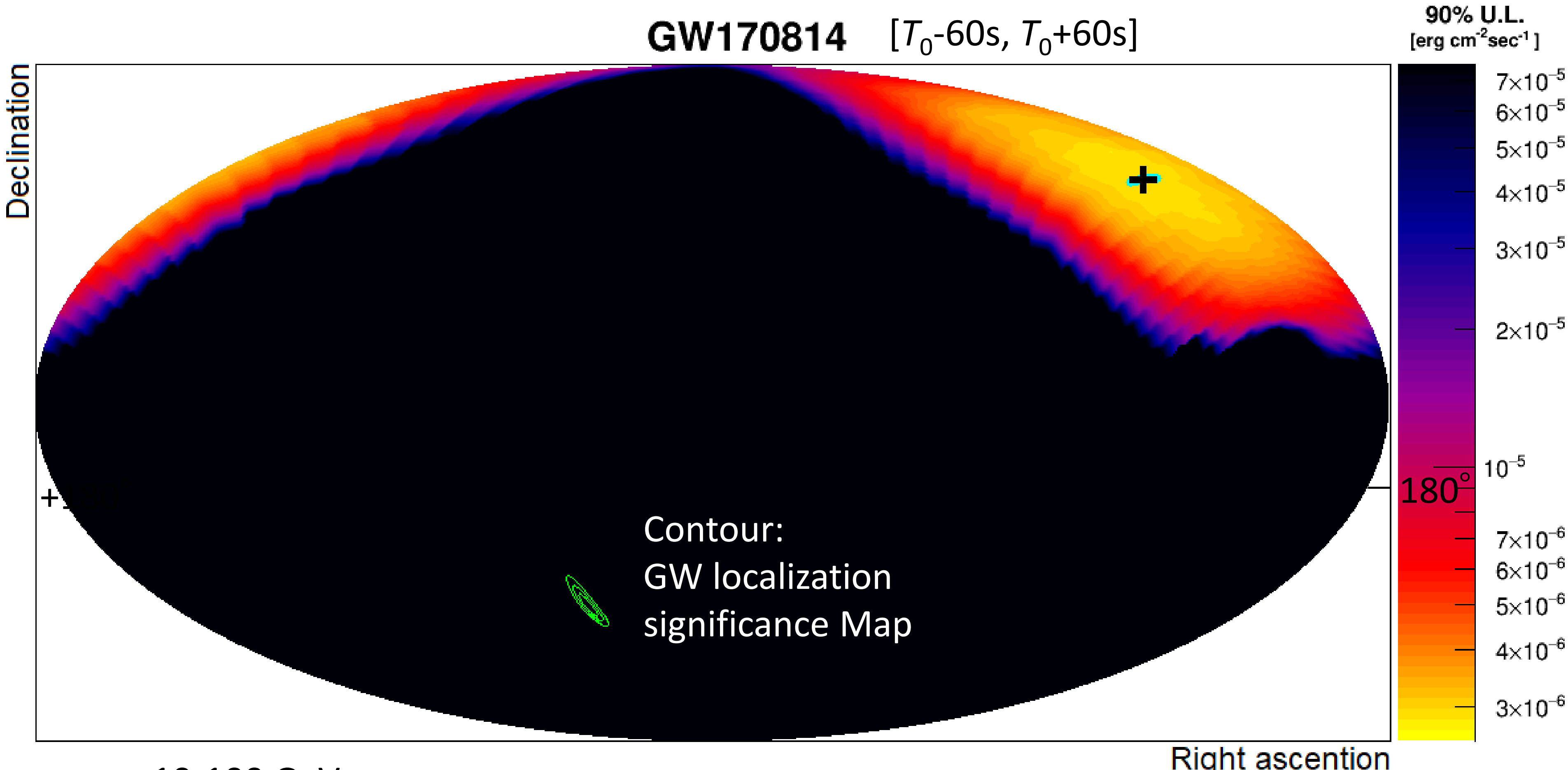

<u>10-100 GeV</u>

No event survived. Backgrounds are negligible.
CALET observation does not constrain any portion of LIGO probability.

90% CL Upper limit for GW170817 counterpart search

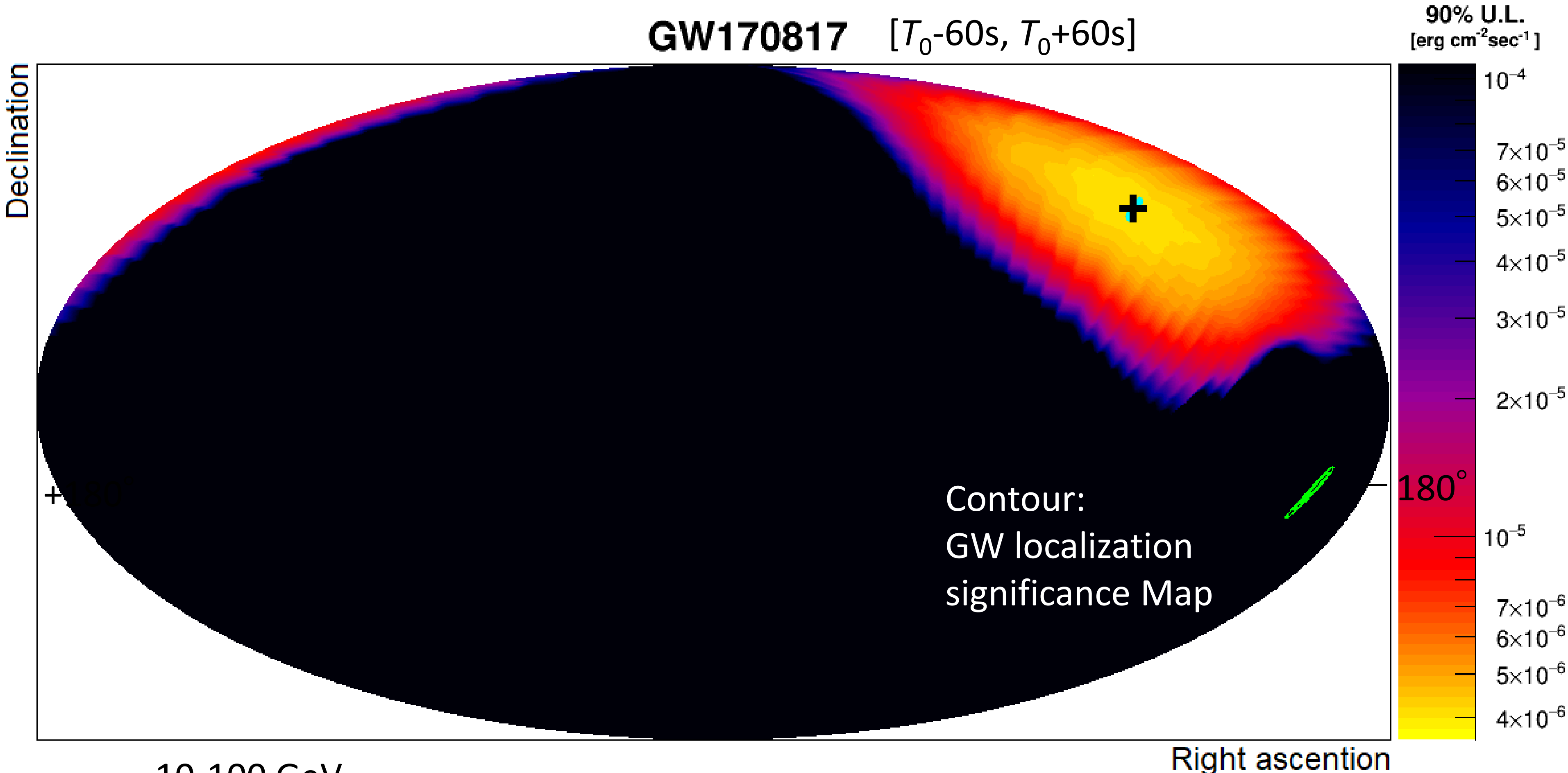

<u>10-100 GeV</u>

No event survived. Backgrounds are negligible.

CALET observation does not constrain any portion of LIGO probability.

CALET Sensitivity to GeV Gamma-Rays

Short GRBs accompanied by GeV gamma-ray emissions could be detected by CALET-CAL given the closeness of GW candidates.

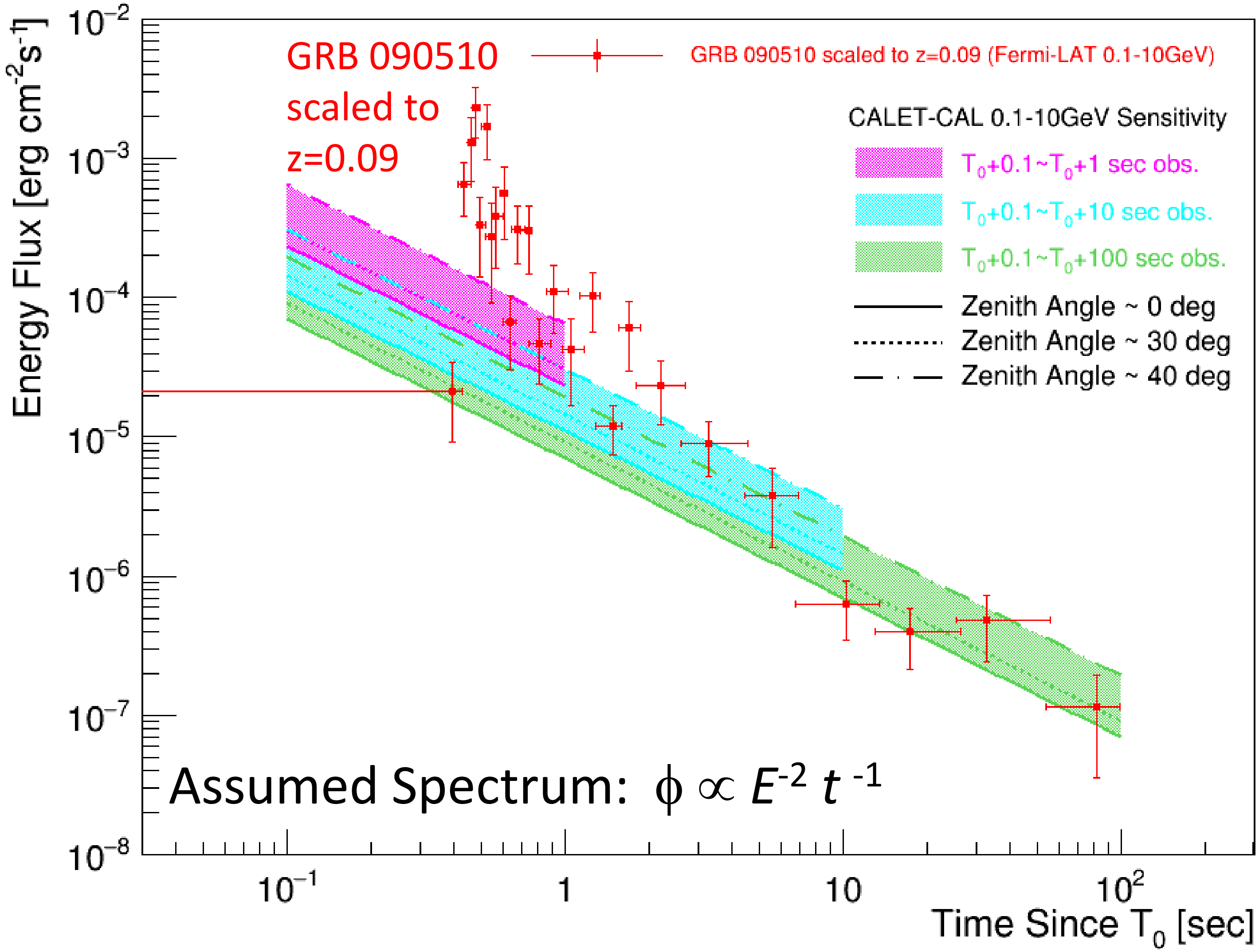

Summary & Prospects

1. **CALET was successfully launched on Aug. 19, 2015, and the detector is being very stable for observation since Oct. 13, 2015.**
2. **As a result of GW151226 counterpart search in GeV gamma-rays, CALET-CAL observation constrains 15% of LIGO localization map by 90% upper limit flux of 9.3×10^{-8} erg cm^{-2}sec^{-1} (1-10GeV).**
3. **GeV gamma-ray counterpart of other GW events during O1&O2 have been performed and limits are set if there is overlap between our FOV and LIGO/Virgo localization map.**
4. **Its sensitivity was validated with diffuse and point-source observations.**
5. **Due to closeness of GW candidates, FOV coverage is more important than deepness of counterpart search assuming on-axis short GRBs as candidates.**
6. **Automated pipeline to search for gamma-ray transients was also developed and is being implemented.**

   ⇒Transient objects such as GW counterparts and GRBs, as well as flaring point sources will be monitored.

This work is partially supported by JSPS Grant-in-Aid for Scientific Research (S) Number 26220708, JSPS Grant-in-Aid for Scientific Research (B) Number 17H02901, JSPS Grant-in-Aid for Scientific Research (C) Number 16K05382.